

Vapor Shield Models for Fusion Reactors Plasma-Facing Components

Nouf AlMousa¹ · Mohamed A. Bourham¹

Published online: 30 June 2016
© Springer Science+Business Media New York 2016

Abstract Radiant heat flux is a dominant mechanism by which energy transfers from the high-temperature core plasma to the interior critical components of the fusion reactor, which result in surface ablation and sever damage to the components. A vapor layer develops at the surface and provides a self-shielding mechanism at the plasma-material interface. Two models for the energy transmission factor through the boundary layer were developed and incorporated in the electrothermal plasma capillary code to predict the effectiveness of these models in surface self-protection. The electrothermal plasma capillary discharge simulates the typical conditions of fusion reactors disruption and quench phase and has been shown to be an adequate technique to evaluate the erosion of plasma-facing component. First model treats the radiant heat transport as it is affected by the variation of the plasma opacity, in which the vapor shield efficiency depends on the plasma optical thickness and the mean plasma opacity. The second model defines the vapor shield by the ratio of the energy reaching the surface to the total radiant energy emitted by the plasma with the inclusion of the plasma kinetic energy. The code can predict the axial and temporal variation of the transmission factor at each time step and mesh point, and predicts the plasma parameters with the effectiveness of the vapor shield at the boundary layer. The code prediction with implementation of both models has been used to compare the results with earlier ones and with some

experimental data. Code results are in good correlation with experimentally measured ablation data.

Keywords Vapor shield plasma · Plasma-surface interface · Electrothermal plasma · Capillary discharges · Disruption high heat flux

Introduction

During off-normal events such as thermal quench phase and hard disruptions in a future tokamak reactor, the plasma facing materials are expected to be exposed to high heat fluxes of up to 100 MJ/m^2 during time scales of 0.1–1 ms. Such high heat fluxes could cause damaging effects due to ablation of the exposed plasma facing surfaces. The exact damage of the exposed surfaces is very critical, hence, many theoretical and experimental studies have been conducted to test the damage of materials exposed to such high heat fluxes. Material erosion studies can be conducted on laboratory devices that produce a tokamak relevant off-normal heat fluxes. Examples of devices that generate powerful heat loads are plasma guns, lasers and electron beam facilities [1]. The material erosion data from such experiments show lower ablation rates compared to expected rates under relevant simulated tokamaks off-normal heat fluxes [2]. For example, data from the VIKA plasma gun experiment predicts ablation rates that are an order of magnitude lower than the estimated values for carbon-based materials in ITER [2]. The decrease in the ablation rate can be explained by the effectiveness of the vapor shield formation at the plasma-material boundary.

Vapor shielding (VS) mechanism results when intense heat fluxes are deposited on solid material surface over

✉ Mohamed A. Bourham
bourham@ncsu.edu

Nouf AlMousa
nalmous@ncsu.edu

¹ Department of Nuclear Engineering, North Carolina State University, Raleigh, NC 27695, USA

short heat-loading periods, which in turn cause sudden evaporation/sublimation of the exposed material. The continuous evaporation forms a vapor cloud adjacent to the solid surface that expands towards the incoming heat flux. Hence, the vapor cloud shields the exposed surface from further evaporation by absorbing a fraction of the incoming heat flux. The exact physics behind the self-shielding mechanism have been discussed in many experimental and theoretical studies in which modeling was limited to consider the vapor shield as a ratio $f = q''_{(at\ surface)} / q''_{(from\ plasma\ core)}$ between the heat flux reaching the surface $q''_{(at\ surface)}$ to the total incoming heat flux $q''_{(from\ plasma\ core)}$ impinging on the surface [1–5]. The accurate evaluation of the effectiveness of the VS is a key problem in predicting the exact damage of solid materials under the impact of high heat fluxes.

Modeling of the VS effect during plasma material interaction (PMI) with the aim of accurate estimation of material erosion is the goal of this study. The VS is formed under the impact of high-density plasma ($\gg 10^{23}/m^3$) and low kinetic plasma temperature ($\ll 100$ eV) for the typical range of electrothermal plasma capillary discharges [1–5]. Such electrothermal (ET) plasma is generated using the NCSU ET facilities, where the ET source produces fast-rise and intense heat fluxes similar to that expected in off-normal events in future large fusion reactors. These facilities (SIRENS and PIPE) each is composed of an ET plasma source and an expansion chamber [4, 5]. The source section consists of high energy density capacitor, a high-voltage high current spark-gap switch, and a capillary that houses an ablative sleeve. The facilities are equipped with various measuring sensors for discharge current and voltage. Detailed description of these facilities is available in the literature [4–7].

In the present work, results from experiments conducted on the PIPE facility are used to compare and validate the proposed VS models. The experiments were carried out using a 340 μ F capacitor that delivers between 1 and 6 kJ of stored energy with discharge currents of 9–43 kA. The corresponding radiant heat flux in these experiments ranges between 10 and 50 GW/m² over duration of 100–150 μ s, which is within the same range expected in future large tokamak fusion reactors. The ablative material used for the capillary lining is a cylindrical tube “sleeve” made of Lexan polycarbonate [C₁₆H₁₄O₃]_n, with 9.0 cm in length and 4.0 mm inner diameter and 8.0 mm outer diameter, which resides inside the main grounded tube-shaped housing of the electrothermal source assembly. The plasma formation within the ET facility has been computationally simulated by the ETFLOWVS code, which is a new version of ETFLOW with incorporation of the newly-developed vapor shield models [7]. Since the objective of this

study is to investigate the VS formation and its effect on the plasma-facing materials, two different VS models were developed and implemented in the code through different subroutines. The implemented subroutines can run individually allowing the flexibility of testing the reliability of each VS model.

Models for Vapor Shielding

The first model, Model 1, is based on simulating the radiant heat transport as it is affected by the variation of the plasma opacity and emissivity. In this model, the calculation of the transmission factor (f) necessitates the evaluation of the VS plasma optical thickness and the mean plasma opacity. For such ET plasma, the Rosseland’s averaging approximation is used for the calculation of the mean plasma opacity. The optical thickness of the VS is calculated and has been found to vary with the radiant heat flux and the density of the vapor cloud.

The second model, Model 2, defines the transmission factor as the ratio of the energy reaching the wall to the total energy emitted towards the wall by the plasma core. The radiative energy transmission factor is found to be strongly dependent on the plasma pressure and density, heat of sublimation/evaporation, the internal energy, and weakly dependent on the plasma kinetic energy.

Vapor Shield Opacity Model “Model 1”

The ideal black body approximation is known to be not accurate enough for modeling kinetic plasma temperatures greater than 1000 K, and hence the near-blackbody, gray-body, approximation is adopted in this model. The heat flux emitted by the plasma as gray-body is a fraction of the blackbody radiation depending on plasma emissivity. Therefore, the total heat flux transported to the material surface can be defined as:

$$H_{rad,gb} = \varepsilon H_{rad,bb} \tag{1}$$

where $H_{rad,gb}$ is the heat flux from the gray-body, and $H_{rad,bb}$ is the heat flux from the blackbody plasma core. The plasma emissivity coefficient is a function of plasma energy and the values can range between 0 and 1. A new term, defined as plasma absorptivity, which measures the fraction of the energy absorbed by plasma is required to determine plasma emissivity. The plasma emissivity can be determined by:

$$\varepsilon = 1 - \exp(-\tau_\omega) \tag{2}$$

where τ_ω is the optical thickness of plasma, which is an important radiation transfer parameter that depends on the

plasma thickness (d) and the absorption coefficient (k'_ω), and can be expressed as:

$$\tau_\omega = \int_0^d k'_\omega dx \quad (3)$$

The optical thickness can determine how the intensity of radiation will be attenuated as it travels from the surface of the vaporized plasma at $x = 0$ and along its bath in the vapor shield layer to reach the ablating wall. The plasma is considered optically thin or transparent when the optical thickness is very small ($\tau_\omega \ll 1$). For quasi-thermal transparent plasma, the total emissivity tends to be equal to the optical thickness such that Eq. 3 can be re-written as:

$$\varepsilon = \tau_\omega \text{ for } \tau_\omega \ll 1 \quad (4)$$

When the optical thickness is large ($\tau_\omega \gg 1$), the plasma will be optically thick or opaque for radiant heat transport.

Electrothermal plasma tends to behave more like a blackbody with total emissivity increases and tends to be closer to its maximum value due to the nature of such plasma with high density, close to local thermodynamic equilibrium (LTE) with isothermal temperature, and has very high optical thickness. This is typical in most ET plasmas where the boundary layer is of higher density compared to the core plasma due to the evolution of additional vaporized mass ablated from the wall surface and forming a thick dense boundary layer. The mathematical consideration to model radiation attenuation within the optically thick plasma necessitates the evaluation of the optical thickness, which is a function of the characteristic length of the medium, and the absorption coefficient. The characteristic length of the boundary layer, the attenuating medium, can be characterized by the effective beam length (L_{eb}), which is the path length in an isothermal homogeneous medium and results in absorption of radiation equal to absorption by the same medium inside the investigated geometry [8]. A new approach has been developed to accurately determine the effective beam length, which relates the effective beam length to the dimension of the region through which the radiation is attenuated. The width of the boundary layer region can be calculated in the code for each mesh point and each time step based on the density of the optically thick plasma. The complexity of having multiple opacity sources at different possibilities depending on the plasma criteria can be solved by an appropriate averaging of the attenuation coefficient. In other words, this can be achieved by computing a mean opacity that is averaged over all frequencies. The Rosseland mean opacity is the most commonly applied approach to find the mean opacity of optically thick electrothermal plasma that met LTE condition [8–10]. The simple expression for one group Rosseland mean opacity (χ_{rav}) as a function of the

frequency-dependent absorption coefficient (χ_v) can be written as:

$$\frac{1}{\chi_{av}} = \int_0^\infty \frac{1}{\chi_v} G'(u) du \quad (5)$$

In this expression the mean opacity is weighted by a weighting function $G'(u)$ given by:

$$G'(u) = \frac{15}{4\pi^4} \frac{u^4 e^{-u}}{(1 - e^{-u})^3} \quad (6)$$

Vapor Shield Energy Ratio Model “Model 2”

A different way to determine the efficiency of the VS is based on the numerical quantification of the transmission factor. In this approach, the transmission factor is determined from the ratio between the two heat fluxes; the heat flux that cause the material erosion (evaporation) to the total heat flux radiated by the plasma core. In this case the incident thermal radiation is assumed to be high enough to directly sublime the impacted material, followed by dissociation and ionization. The relationship between the dissociation energy E_D and the sublimation energy (H_{sub}) is expressed as $E_D = m_p H_{sub}$ where m_p is the atomic mass of the constituent atoms. In addition to the sublimation energy, other resources can determine the total energy of the plasma species, specifically the density of the evaporated material (ρ) and the kinetic pressure of the plasma (P). Hence, the transmission factor is calculated according to the previous definition of heat fluxes and can be written as [7–9]:

$$f = \frac{\rho H_{sub}}{P + \rho H_{sub} + \rho U} \quad (7)$$

The internal energy is due to sublimation energy, ionization potential (\bar{I}), and the thermal motion and for ideal plasma can be expressed as $U = 1.5 KT(1 + \bar{Z}) + \bar{I} + H_{sub}$ where \bar{Z} is the average charge state [7–10]. An additional term ($\frac{1}{2}mv^2$) has been added in the denominator of Eq. (7) to account for kinetic energy, which can lead to lower energy transmission factor and hence less heat flux to reach the surface resulting in a prediction of less ablation.

Results and Discussion

ETFLOWVS code with the developed VS models has been used to study the erosion of the plasma facing material with the effect of the vapor shield. For a given ET source geometry and initial discharge parameters the code calculates the initiation of the plasma followed by calculation of

the plasma temperature, heat flux, density, pressure, ablated mass, and velocity with detailed calculation of the number density of electrons and ions (up to the second ionization) and the neutrals. The input discharge current into the code is an experimentally measured one taken from the experimental facility PIPE. The detailed composition and the plasma species distribution are determined from subroutines that solve a linearized Saha equation and a linearized equation of state. The set of governing equations are linearized and discretized by integrating over a finite control volume with an assumption of spatially constant plasma. The resulting set of linear differential equations with the appropriate boundary conditions is solved using Newton's method finite difference approximation [7, 9, 11]. The mesh spacing and time step values were chosen to optimize the computational run time and the accuracy of calculations. The bulk plasma parameters are computed for each mesh point at each time step and are manipulated at the next time step to find the solution for new plasma parameters as time progresses.

Figure 1 represents the shapes of the discharge currents used in this study where all current pulses are the actual discharge currents recorded from experiments conducted on the PIPE facility [7, 11]. Although the code can generate any form of discharge current with any desired peak and pulse length, however, it is an advantage to use experimentally measured currents instead of artificially generated current profiles. This choice avoids discrepancy between computational and experimental results that may arise due to employing negotiable theoretical models and simplifying assumption that might not perfectly fit the physics of the case study. The selected discharge currents peak between 9 and 43 kA over a discharge duration of 100–150 μs for a discharge arc voltage range between 1 and 5 kV. These shots were also validated between the

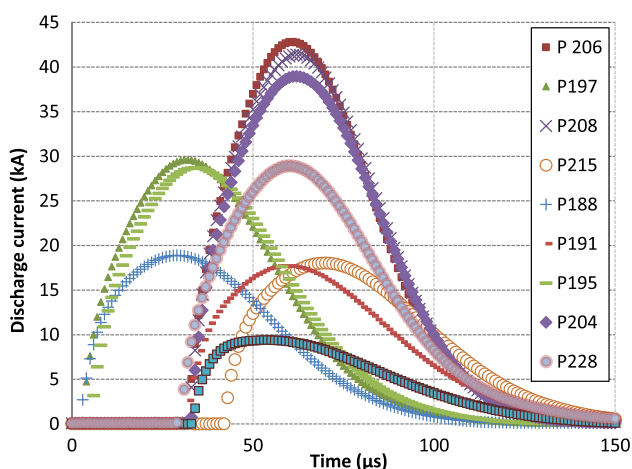


Fig. 1 Recorded discharge current from the PIPE electrothermal plasma facility

code and the measurements of the total ablated mass and hence their selection for the study is adequate and beneficial for the evaluation of the new vapor shield model. The ETFLOWVS code reads the input file of the discharge current and runs the case for the selected sleeve material. The material data in this case study is Lexan polycarbonate ($\text{C}_{16}\text{H}_{14}\text{O}_3$), which is automatically imported with its parameters from the materials library that is built in ETFLOWVS code.

Four test cases have been run using the developed vapor shield models and the results are compared to the experimentally measured ablated mass as available measured data. The four test cases are cases that used Model 1 “Opacity model”, Model 2 “Ratio model”, a modified Model 2 “Ratio with kinetic energy”, and a fully transparent vapor shield where the transmission factor equals unity.

Figure 2 shows the measured total ablated mass as a function of the peak discharge current as recorded from the actual PIPE shots [7, 11]. The energy discharged during the shots for this study has been classified to three regimes, low, medium, and high discharge energy. Figure 2 shows a comparison between the calculated total ablated mass using various VS models and the experimentally measured values. There is a strong dependence of the total ablated mass on the magnitude of the discharge current due to the fact that any increase in the discharge current results in an increase in the radiant heat flux from the core plasma regardless of the adopted VS model. The dependence on the peak value of the discharge current follow the same trend for the measured ablated mass showing an increase with the increase of the current magnitude. The non-vapor shield calculations overestimate the total ablated mass compared to the experimentally measured values. This can be explained by the assumption that the entire radiant heat flux from the plasma core is deposited on the exposed surface without any vapor shielding.

Increased overestimation is observed towards the higher discharge current range, suggesting that there is an increase in the vapor shield efficiency as the incident radiant heat flux increases. Furthermore, it can also be seen from Fig. 2 that the total ablated mass calculated by the developed VS models lie within the range set by the margin of error of 10 % of the measured ablated mass. However, in the lower current range, both VS models predicted values are lower than the measured ones and fall out of the defined error margin. The off normal behavior of some low energy shots was due to broken, fragmented, cracked and deformed samples and the possibility of forcing the sample outside the source inner tubing [7, 11]. Excluding the low current shots, there is a good agreement between experimental and simulation data by using the developed VS models.

Fig. 2 Total ablated mass as a function of the peak discharge current

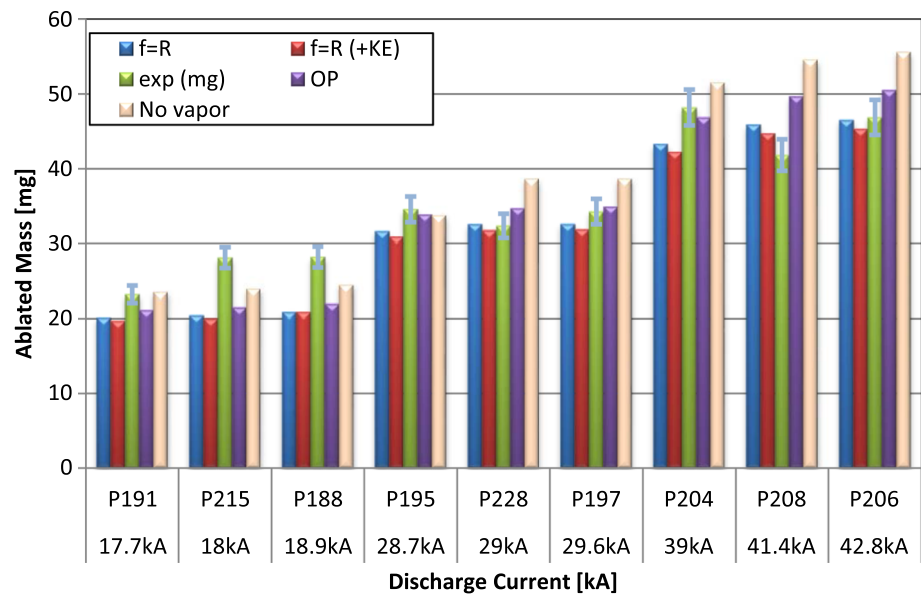


Fig. 3 Plasma density as a function of the peak discharge current for all VP models

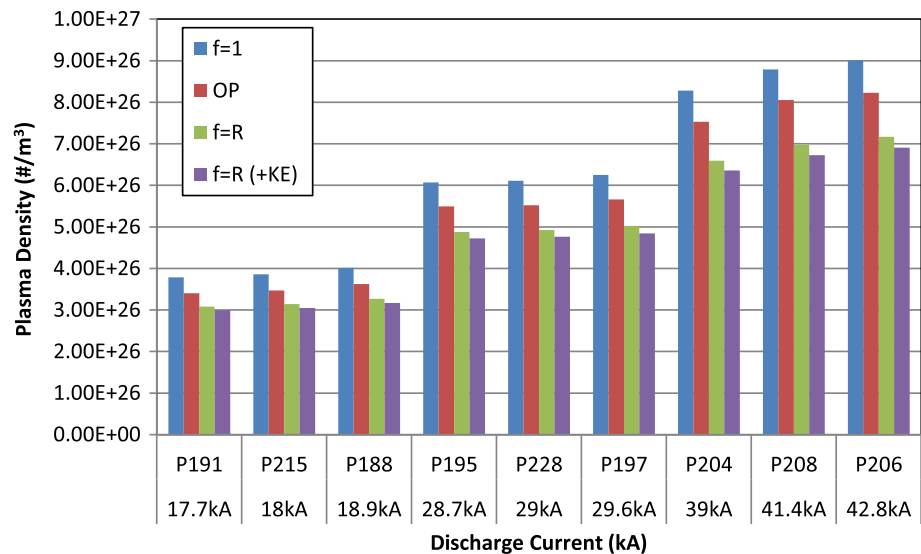
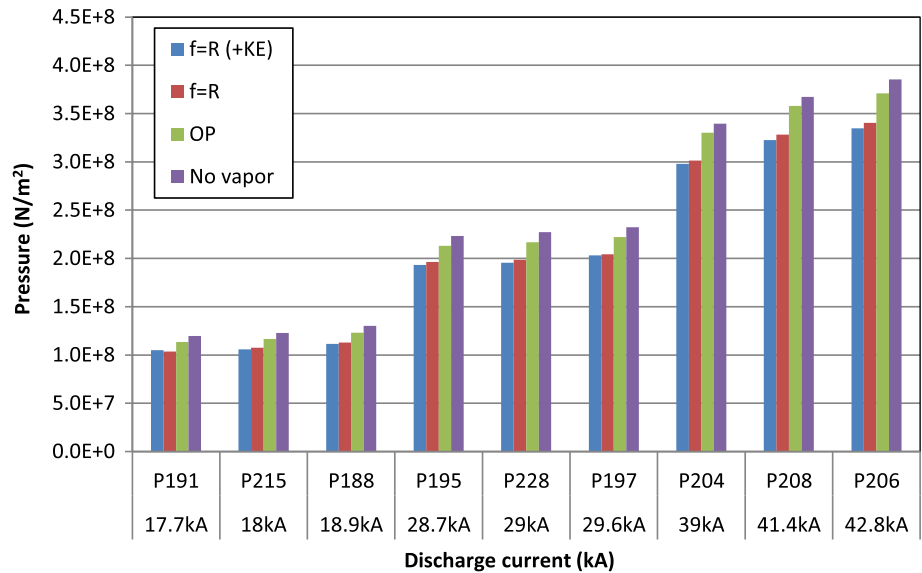


Figure 3 shows the code results for the plasma total number density as calculated by the various VS models. The assumption of no vapor shield ($f = 1$) indicates the highest density as it is attributed to the full energy deposition on the surface without vapor shield. The opacity and ratio models show less plasma density as a result of less ablation due to the effectiveness of the vapor shield. The ratio model with the inclusion of the kinetic energy “ $f = R + (KE)$ ” shows the lowest density, which shows that the plasma density decreases by about 20.5 % on average when using this model. The opacity model ($f = OP$) result falls between the ratio model ($f = R$) and the no vapor shield model ($f = 1$), with about 8.5 % decrease in the plasma density. It indicates that the opacity

is an attenuation effect as modeled by an exponential decay model, and that the developed boundary layer is determined by the boundary layer thickness. Of importance is that the model assumed a mean opacity that is averaged over all frequencies. From all models, it is clear that the vapor shield provides a self-protecting mechanism to the surface.

Figure 4 compares the plasma pressure results using the different VS models. The pressure is determined by the equation of state $P = nkT(1 + \bar{Z})$ where n is the plasma number density; kT is the plasma kinetic temperature and \bar{Z} is the average charge state [12, 13]. Accordingly, it is expected that the pressure results will be influenced by the plasma density results. However, a modification of the

Fig. 4 Plasma pressure as a function of the peak discharge current for all VS models

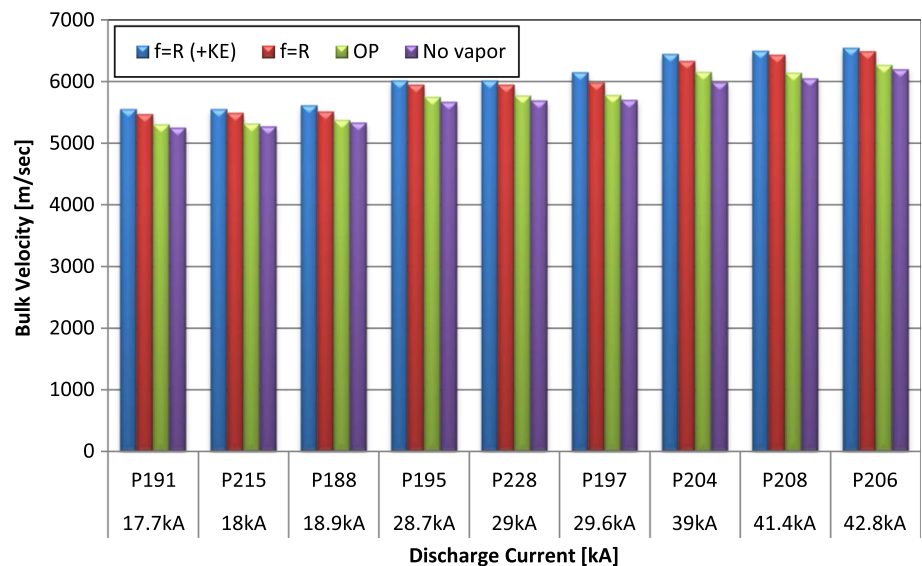


equation of state to account for the long-term Coulomb interactions necessitates the addition of a pressure correction term $\Delta P = kT/24\pi\lambda_D^3$ where λ_D is the Debye length, and hence the equation of state is modified to $P + \Delta P = \sum nkT$ which takes into consideration such pressure corrosion [7, 12–15].

Results of the Model 1 “Opacity model” suggests that the developed optically thick vapor layer results in a pressure reduction of 4.3 % compared to non-vapor shield calculations, and Model 2 ‘Ratio model’ shows an average of 12.5 % reduction in the pressure. As seen in Fig. 4, the effect of the plasma species kinetic energy on the plasma pressure is small for low current ranges, however, the effect is getting more pronounced with the increase in the magnitude of the discharge current.

Unlike the plasma density and pressure, the plasma bulk velocity decreases compared to the case where no VS formation is taking place, which is an expected result regardless of which vapor shield model was adopted [16]. As seen in Fig. 5, Model 1 “Opacity model” shows velocity values a bit higher than that without vapor shield, almost 1 %, which indicates that the optically thick vapor layer does not seem to strongly affect the bulk plasma motion. On the other hand, Model 2 “Ratio model” predicts plasma velocities that are over 5 % greater than those in absence of VS. Comparing Model 2 “Ratio model” calculations with and without kinetic energy consideration has shown that the inclusion of the plasma kinetic energy results in a better vapor shielding effect. This can be attributed to the effect of allowing the kinetic energy of the

Fig. 5 Plasma bulk velocity as a function of the peak discharge current



impinging plasma species to contribute to the total incident power density, which slightly decreases the transmission factor meaning that higher shielding can be provided by the boundary layer.

In the subsequent section, PIPE shot number P228 has been chosen to further investigate the vapor shield parameters as a sample shot, however, similar trends would be expected in the rest of the other shots. This shot was chosen as it represents the mid-range discharge energy among all shots presented in this study. It is also of a record that it is a clean experimental shot with ablated mass that matches the simulation values calculated by both models.

All above calculations by the proposed VS models differ in the way the transmission factor is calculated based on the modeling of the VS evolution. Shown in Fig. 6 is the temporal evolution of the transmission factor for an

incident discharge current that peaks at 29 kA as predicted by ETFLOWVS vapor shield models.

The temporal behavior of the plasma parameters, temperature, density, heat flux and pressure, follow the temporal behavior of the discharge current. This, consequently, implies that the time variation of the deposited energy and the evolved VS layer on the exposed surface forces a temporal variation in the energy transmission factor, and hence in the boundary layer behavior. The theory adopted for Mode 1 “Opacity”; an optically thick VS forms and builds up on the surface due to the exposure to the incident high heat flux from the plasma core. As a result, the transmission factor is exponentially decreasing over the course of energy deposition despite the after-peak decreasing current and input power. This is caused by the formation of the optically thick boundary layer as its opacity plays a significant role to exponentially attenuate the transmission of the incoming radiant heat flux from the photons and plasma particles.

However, the predicted temporal evolution by Mode 2 “Ratio” of the transmission factor is completely different. As per this model, the transmission factor drops rapidly from its initial value of unity as the deposited discharge energy increases up to its peak. Soon after the beginning of the discharge, the transmission factor reaches a minimum value of 0.6 for the rest of the 120 μ s discharge time; the transmission factor gradually increases to about 0.9 due to reduced plasma heat flux as the input power decreases. Also, as seen in Fig. 6, the transmission factor follows an inverse profile of the typical temporal evolution of the discharge current as predicted by this model.

Figure 7 supports the earlier findings in regard to radiation attenuation by optically thick vapor shield (a thicker boundary layer). The optical thickness of the boundary

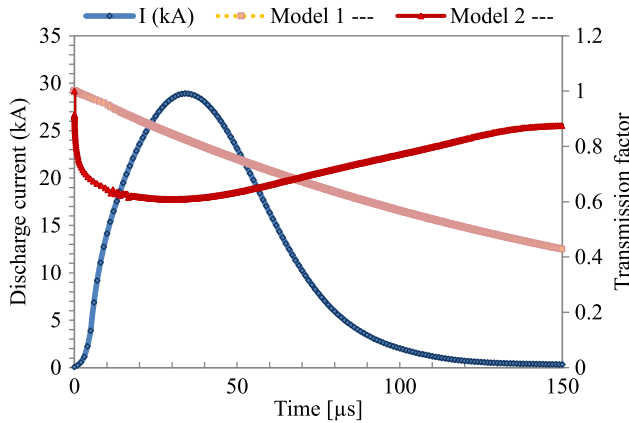


Fig. 6 Temporal evolution of the transmission factor for a 29 kA discharge current

Fig. 7 Variation of the optical thickness of the boundary layer and the transmission factor as functions of discharge time

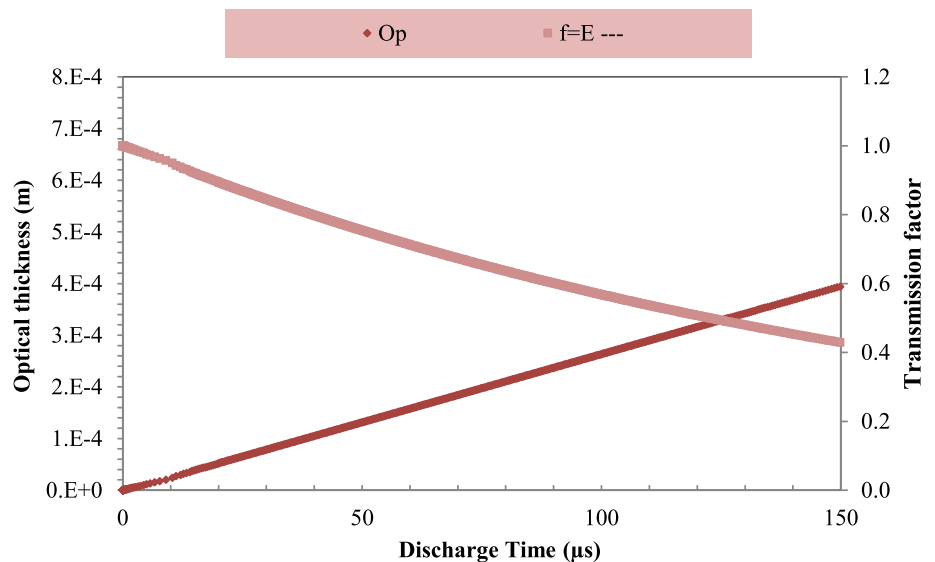
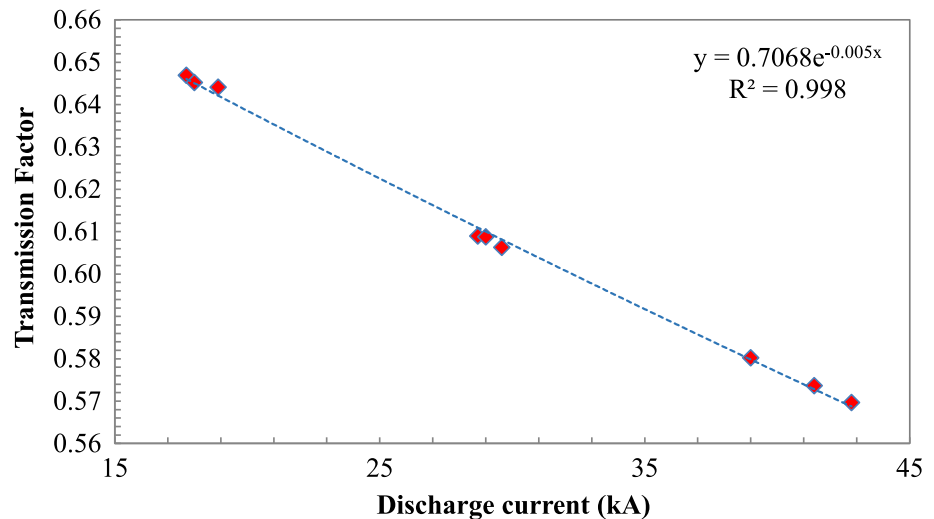


Fig. 8 Value of the transmission factor (f_{\min}) as a function of the discharge current



layer has a great impact on the transmission factor as shown on Fig. 7. The optical thickness increases as thicker boundary layer accumulates over the exposed surface. The increasing optical thickness strongly indicates stronger attenuation of the transmitted radiant heat flux through the boundary layer. As mentioned earlier, the attenuation in this model accounts for all possible radiation absorption processes upon the formation of the optically thick boundary layer, the transmission factor exponentially decaying to a minimum value despite the cooling down of the bulk plasma at the end of the discharge.

The values of the transmission factor as a function of the discharge current is shown in Fig. 8. The transmission factor drops exponentially with the increase in the magnitude of the discharge current. For Lexan polycarbonate material, it varies from 0.65 to 0.56 for the discharge current range between 15 and 45 kA, respectively. The data in Fig. 8 indicates better shielding by the VS with the increase in the input power, and consequently the increase in the incident radiant heat flux. This is primarily due to the increased sublimed material that forms the absorbing boundary layer.

Conclusions

Calculations of the transmission factor at each time step and mesh point have been conducted with the ET code ETFLOWVS to predict the plasma parameters at the capillary exit and the mass ablated from the capillary inner wall. The code predictions were used to compare the results of two newly-developed vapor shield models with earlier ones and with experimental data of mass ablation from an ET source. The inclusion of the vapor shield modeling produces less deviation from the measured

ablated mass as compared to earlier calculations. However, the plasma bulk has higher exit velocities by including the vapor shield effect. The conducted calculation using Model 1 “the opacity model” has shown that the energy transmission factor through the vapor shield for Lexan varies with the peak discharge current. The calculations using Model 2 “the ratio model” suggests that the optical thickness of the vapor shield varies with the incident radiant heat flux. Code results for Lexan polycarbonate indicate a transmission factor of 0.65 to 0.56 for the discharge current range between 15 and 45 kA, respectively, which confirms a reduction in the energy reaching the surface as the initial energy deposition from the plasma core increases. This self-protecting mechanism, the vapor shield at the plasma-surface interface, is an essential mechanism in reducing surface erosion from incoming high heat flux, and indicates that all tested models are providing such protection. The essential vapor shield mechanism is of important applicability in future fusion tokamak reactors where plasma facing materials are expected to suffer from high heat flux deposition.

References

1. A. Hassanein, I.K. Konkashbaev, Disruption simulation experiments and extrapolation to reactor conditions. In: *Proceedings of 20th Symposium on Fusion Technology (SOFT-20)*, Marseilles, France, 7–11 September (1998)
2. A. Hassanein, G. Federici, I. Konkashbaev, A. Zhitluknin, V. Litunovsky, Materials effects and design implications of disruptions and off-normal events in ITER. *Fusion Eng. Des.* **39–40**, 201–210 (1998)
3. N.N. Ogurzowa, I.V. Podmoshenskii, P.N. Rogovtsev, Calculation of the parameters of an optically dense plasma obtained by a discharge with an evaporating wall. *High Temp.* **9**, 430–435 (1971)

4. J. Gilligan, M. Bourham, O. Hankins, W. Eddy, J. Hurley, D. Black, Vapor shield protection of plasma facing components under incident high heat flux. *J. Nucl. Mater.* **196–198**, 596–601 (1992)
5. M. Bourham, O. Hankins, O. Auciello, J. Stock, B. Wehring, R. Mohanti, J. Gilligan, Vapor shielding and erosion of surfaces exposed to a high heat load in an electrothermal accelerator. *IEEE Trans. Plasma Sci.* **17**, 386–391 (1989)
6. W. Oberle, I. Stobie, M. Del Guercio, K. White, M. Bourham, J. Gilligan, *Summary of Experimental Efforts to Determine Plasma-Augmented Burn Rates for Solid Propellants*. Army Research Laboratory, Adelphi, MD, ARL-TR-782, Final Report, June (1995)
7. L. Winfrey, M.A. Abd Al-Halim, J.G. Gilligan, A.V. Saveliev, M.A. Bourham, A study of plasma parameters in a capillary discharge with calculations using ideal and nonideal plasma models for comparison with experiment. *IEEE Trans. Plasma Sci.* **40**, 843–852 (2012)
8. J.D. Powell, A.E. Zielinski, Capillary discharge in the electrothermal gun. *IEEE Trans. Magn.* **29**, 591–595 (1993)
9. J. Hurley, M. Bourham, J. Gilligan, Numerical simulation and experiment of plasma flow in the electrothermal launcher SIRENS. *IEEE Trans. Mag.* **31**, 616–621 (1995)
10. J.G. Gilligan, R.B. Mohanti, Time-dependent numerical simulation of ablation-controlled arcs. *IEEE Trans. Magn.* **18**, 190–197 (1990)
11. H.C. Hottel, A.F. Sarofim, *Radiative Transfer* (McGraw-Hill, New York, 1967)
12. Y.B. Zel'dovich, Y.P. Raizer, *Physics of Shock Waves and High-Temperature Hydrodynamic Phenomena*, vol. 1 (Academic Press, New York, 1966)
13. H.G. Griem, High-density corrections in plasma spectroscopy. *Phys. Rev.* **128**, 997–1003 (1962)
14. *Hydrodynamic Phenomena*, vol. 1 (Academic Press, New York and London, 1966)
15. M.R. Zaghoul, Improved modelling of electrothermal plasma source with radiation transport. *J. Phys. D Appl. Phys.* **41**, 1–10 (2008)
16. N. AlMousa, L. Winfrey, J. Gilligan, M. Bourham, Radiative heat transport through vapor plasma for fusion heat flux studies and electrothermal plasma sources applications. *J. Nucl. Energy Sci. Power Gener. Technol.* **3**, 1–7 (2014)